Catalysis Today 142 (2009) 272–277

Contents lists available at ScienceDirect

Catalysis Today

journal homepage: www.elsevier.com/locate/cattod

Selective oxidation of ethane: Developing an orthorhombic phase in Mo–V–X (X = Nb, Sb, Te) mixed oxides

P. Botella [a], A. Dejoz [b], M.C. Abello [c], M.I. Vázquez [b], L. Arrúa [c], J.M. López Nieto [a,*]

[a] Instituto de Tecnología Química, UPV-CSIC, Avda. Los Naranjos s/n, 46022 Valencia, Spain
[b] Departamento de Ingeniería Química, Universidad de Valencia, Dr. Moliner 50, 46100 Burjassot, Spain
[c] Instituto de Investigaciones en Tecnología Química (UNSL-CONICET), Chacabuco y Pedernera, C.C. 290, 5700 San Luis, Argentina

ARTICLE INFO

Article history:
Available online 4 November 2008

Keywords:
Oxidative dehydrogenation
Ethane
Ethene
Mixed metal oxides catalyst
Mo–V–Nb
Mo–V–Sb
Mo–V–Te–Nb
Catalyst characterization

ABSTRACT

Mo–V–X (X = Nb, Sb and/or Te) mixed oxides have been prepared by hydrothermal synthesis and heat-treated in N_2 at 450 °C or 600 °C for 2 h. The calcination temperature and the presence or absence of Nb determines the nature of crystalline phases in the catalyst. Nb-containing catalysts heat-treated at 450 °C are mostly amorphous solids, while Nb-free catalysts heat-treated at 450 °C and samples treated at 600 °C clearly contain crystalline phases. TPR-H_2 experiments show higher H_2-consumption on catalysts with amorphous phases. Catalytic results in the oxidative dehydrogenation of ethane indicate that the selective production of the olefin is strongly related to the development of the orthorhombic $Te_2M_{20}O_{57}$ or $(SbO)_2M_{20}O_{56}$ (M = Mo, V, Nb) phase (the so-called M1 phase), which is mainly formed at 600 °C. This active and selective crystalline phase is characterized to show moderate reducibility and active centers enough for the selective oxidative activation of ethane with the minimum quantity possible of active centers for ethylene activation. In this sense, the best yield to ethylene has been achieved on a Mo–V–Te–Nb mixed oxide.

1. Introduction

During the last two decades many investigations have been conducted to the application of mixed metal oxides with reducible metal oxides as catalysts for the selective oxidation of short chain alkanes [1–17]. These materials work at temperatures below 600 °C through a Mars van Krevelen mechanism. For this reason the reducibility should have an important influence on their catalytic behavior.

In the case of the oxidation of ethane, Mo–V–Nb mixed oxides undoped or doped with Sb, formerly proposed by Union Carbide Corp., were found useful for the oxidative dehydrogenation of ethane to ethylene (ODH) at 400 °C with high efficiency [9–11], with a yield of the olefin above 50% in the best catalyst $Mo_{0.62}V_{0.26}Nb_{0.07}Sb_{0.04}Ca_{0.01}$ [11]. After these results, an intense study on MoVNb materials was carried out, although without greater improvements in the catalytic performance [12–19]. But in all cases, their catalytic performance is strongly related to the catalyst composition.

Recently, it has been shown that Mo–V–Te–Nb mixed oxides present an outstanding activity and selectivity in the ethane ODH [20,21]. The catalysts, heat-treated in N_2 at 600–650 °C, allow to obtain an ethylene yield of about 75% [20], which has been related to the presence of orthorhombic $Te_2M_{20}O_{57}$ phase (the so-called M1 phase, M = Mo, V, Nb) [21]. In parallel to this, it has been proposed that MoVSbO catalysts are also very selective in the ethane ODH when the catalyst presents the orthorhombic $(SbO)_2M_{20}O_{56}$ phase (isomorphous to $Te_2M_{20}O_{57}$) [22]. These catalysts were initially proposed for the (amm)oxidation of propane [4–8,23–28].

In this work we present a comparative study on the influence of both the composition and the activation temperature of catalysts on the catalytic performance in the ethane ODH of catalysts based in Mo–V–X mixed oxides (X = Nb, Te, Sb). In this sense, we have compared four mixed oxides catalysts with high selectivity to ethylene [21–23], i.e. Mo–V–Nb–O, Mo–V–Sb–O, Mo–V–Te–O and Mo–V–Te–Nb–O. The catalysts have been heat-treated at 450 °C or 600 °C in N_2 before the catalytic test. The development of an active and selective crystalline phase and the modification of the catalyst reducibility have been proved to be crucial factors on the catalytic performance of these types of materials in the ethane ODH.

* Corresponding author. Fax: +34 96 3877809.
E-mail address: jmlopez@itq.upv.es (J.M. López Nieto).

0920-5861/$ – see front matter © 2008 Elsevier B.V. All rights reserved.
doi:10.1016/j.cattod.2008.09.016

2. Experimental

2.1. Catalyst preparation

Four series of mixed oxides based on Mo–V–X (X = Nb, Sb, Te) have been synthesized according to previously described recipes [13,21–23]. The starting aqueous gel of Mo, V, Nb, Sb and/or Te salts was heated in hydrothermal conditions at 175 °C for 48–96 h. The obtained solids were filtered off, washed with distilled water and dried at 100 °C overnight, and finally heat-treated in N_2 at 450 °C or 600 °C for 2 h. According to the element incorporated in the Mo–V-mixed oxides structure we have four different series of catalysts: A-series (X = Nb), B-series (X = Sb), C-series (X = Te) and D-series (X = Te and Nb). Depending on the heat-treatment temperature we distinguish among catalysts X-450 or X-600 (for catalysts heat-treated at 450 °C or 600 °C, respectively). The characteristics of catalysts are shown in Table 1.

2.2. Catalyst characterization

Bulk composition of all the samples was determined by atomic absorption spectroscopy (AAS) and inductive coupled plasma (ICP). BET specific surface areas were measured on a Micromeritics ASAP 2000 instrument (Kr adsorption) and on a Micromeritics Flowsorb instrument (N_2 adsorption). X-ray diffraction patterns (XRD) were collected using a Phillips X'Pert diffractometer equipped with a graphite monochromator, operating at 40 kV and 45 mA and employing nickel-filtered Cu Kα radiation (λ = 0.1542 nm). Diffuse reflectance UV–vis spectra (DRS) were collected on a Cary 5 apparatus equipped with a 'Praying Mantis' attachment (from Harric) under ambient conditions. $TeMo_5O_{16}$, MoO_3, MgV_2O_6, V_2O_5, H_6TeO_6, TeO_2, Sb_2O_3, SbO_2 and Sb_2O_5 have been used as standard compounds [22,24].

Temperature programmed reduction (TPR) experiments were carried out on 12–18 mg of catalyst with a N_2:H_2 flow (5% H_2, 56.9 μmol_{H_2} min^{-1}) in the temperature range of 100–700 °C, and a heating rate of 10 °C min^{-1}.

2.3. Catalytic testing

The catalytic experiments were carried out under steady-state conditions using a fixed bed quartz tubular reactor working at atmospheric pressure. The flow rate (25–100 ml min^{-1}) and the amount of catalyst (0.5–2.0 g, 0.3–0.5 mm particle size) were varied in order to achieve different ethane conversions. The feed consisted of a mixture of ethane/oxygen/helium with a molar ratio of 30/20/50. Experiments were carried out in the 340–400 °C temperature range. Reactants and reaction products were analysed by on-line gas chromatography, using two columns [21]: (i) Porapak QS (2.0 m × 1.8 in.) to separate CO_2 and hydrocarbons; (ii) Carbosieve-S (2.4 m × 1.8 in.) to separate O_2 and CO.

3. Results and discussion

3.1. On the catalyst characterization

Characteristics of catalysts are shown in Table 1. It can be seen that the temperature treatment (450 °C or 600 °C) does not have any significant influence on the final composition of the catalyst. However, materials heat-treated at 450 °C present BET surface areas clearly higher than those observed for catalysts heat-treated at 600 °C. On the other hand, the heat-treatment temperature has a high influence over the type and amount of the phases formed.

Fig. 1 shows the XRD patterns of heat-treated catalysts at 450 °C and 600 °C. In the case of A-series, i.e. MoVNbO catalysts (Fig. 1, patterns a and b), the heat treatment at 450 °C leads to a low crystalline precursor similar to those reported by other authors in air calcinations at 400 °C [9–14], corresponding to V- or Nb-doped sub-oxides of MoO_3. However, calcination at 600 °C allows the formation of several θ-Mo_5O_{14} derivative crystalline phases, due to partial substitution of Mo by V and/or Nb, i.e. $(Mo_{0.93}V_{0.07})_5O_{14}$ and $(Mo_{0.91}Nb_{0.09})O_{2.80}$ (although the presence of a mixed phase $Mo_{5-x}(V,Nb)_xO_{14}$ should also be considered) [12,14]. Besides this, the presence of $3MoO_2{\cdot}Nb_2O_5$ and MoO_2 have also been detected.

XRD patterns of B-series, i.e MoVSbO catalysts (Fig. 1, patterns c and d), show a behavior with calcination temperature different to those observed in A-series. Although the material heat-treated at 450 °C presents low crystallinity, reflexions at 2θ = 7.8°, 8.9°, 22.1°, 27.1°, 29.3°, 30.5° and 35.3° indicate the presence of $(SbO)_2M_{20}O_{56}$ (M = Mo, V), whereas the diffraction peaks at 2θ = 22.1°, 28.2°, 36.2° and 45.0° are related with $(Sb_2O)M_6O_{18}$ [25]. However, the treatment at 600 °C of this material allows the improvement of crystallinity of both phases (Fig. 1, pattern d), although probably with a significant development of the M2-type phase, (Sb_2O)-Mo_6O_{18}.

Similar XRD patterns are observed in the case of C-series, i.e. MoVTeO catalysts (Fig. 1, patterns e and f). In this case, the sample heat-treated at 450 °C is highly crystalline and main reflexions at 2θ = 7.6°, 8.6°, 12.2°, 13.8°, 16.4°, 22.1°, 23.5°, 24.8°, 26.1°, 27.0°, 29.1°, 30.4°, 31.5° and 35.3° indicate the presence of $Te_2M_{20}O_{57}$ (M = Mo, V) [26–29]. Conversely, the appearance of intense peaks at 2θ = 28.2°, 36.2° and 45.0° in the sample heat-treated at 600 °C indicate the presence of $Te_{0.33}MO_{3.33}$ (M = Mo, V) [24,27,29], whereas the sharp peak at 2θ = 24.9° corresponds to the formation of some θ-Mo_5O_{14} derivative crystalline phases, probably by partial decomposition of the major M1- and M2-type phases.

The incorporation of Nb in the Mo–V–Te mixed oxides leads to important structural changes (Fig. 1, patterns g and h). The solid heat-treated at 450 °C is practically amorphous, with a similar pattern to that observed for Te-free sample. Nevertheless, the heat-treatment at 600 °C leads to the development of $Te_2M_{20}O_{57}$ (M = Mo, V, Nb) as the main crystalline phase, with a scarce presence of the $Te_{0.33}MO_{3.33}$ (M = Mo, V, Nb) phase. On the other hand, it is

Table 1
Chemical and physical properties of heat-treated Mo–V–X catalysts (X = Nb, Sb, Te).

Catalyst	S_{BET} (m^2 g^{-1})	Chemical composition[a]	H_2-uptake in TPR ($mmol_{H_2}$ g_{cat}^{-1})	XRD phases
A-450	25.2	$Mo_1V_{0.10}Nb_{0.19}O_x$	3.97	Amorphous
A-600	24.3	$Mo_1V_{0.07}Nb_{0.15}O_x$	4.61	$(Mo_{0.93}V_{0.07})_5O_{14}$/$(Mo_{0.91}Nb_{0.09})O_{2.80}$, $3MoO_2{\cdot}Nb_2O_5$
B-450	15.3	$Mo_1V_{0.18}Sb_{0.18}O_x$	5.98	$(SbO)_2M_{20}O_{56}$ > $(Sb_2O)M_6O_{18}$
B-600	9.5	$Mo_1V_{0.19}Sb_{0.16}O_x$	5.75	$(SbO)_2M_{20}O_{56}$, $(Sb_2O)M_6O_{18}$
C-450	8.0	$Mo_1V_{0.51}Te_{0.16}O_x$	7.55	$Te_2M_{20}O_{57}$ ≫ $Te_{0.33}MO_{3.33}$
C-600	6.8	$Mo_1V_{0.43}Te_{0.18}O_x$	5.53	$Te_2M_{20}O_{57}$, $Te_{0.33}MO_{3.33}$ > $(Mo_{0.93}V_{0.07})_5O_{14}$
D-450	23.1	$Mo_1V_{0.21}Te_{0.21}Nb_{0.18}O_x$	4.79	Amorphous
D-600	9.1	$Mo_1V_{0.20}Te_{0.18}Nb_{0.21}O_x$	4.50	$Te_2M_{20}O_{57}$ ≫ $Te_{0.33}MO_{3.33}$

[a] Atomic ratio in calcined samples, determined by AAS and ICP.

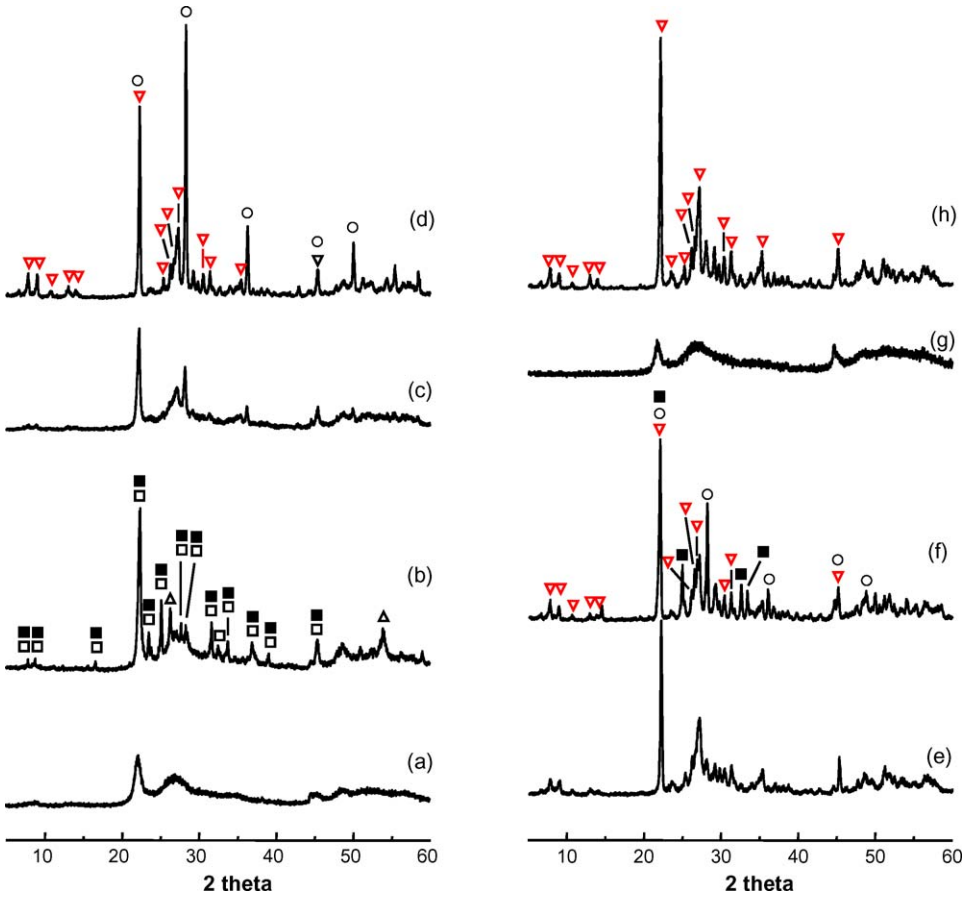

Fig. 1. XRD patterns of catalysts: (a) A-450; (b) A-600; (c) B-450; (d) B-600; (e) C-450; (f) C-600; (g) D-450; (h) D-600. *Symbols*: $3MoO_2{\cdot}Nb_2O_5$ (□); $(Mo_{0.93}V_{0.07})_5O_{14}$ and/or $(Mo_{0.91}Nb_{0.09})O_{2.80}$ (■); MoO_2 (△); M1-type phase ($Te_2M_{20}O_{57}$ or $(SbO)_2M_{20}O_{56}$) (M = Mo, V, Nb) (▽); M2-type phase ($Te_{0.33}MO_{3.33}$ or $(Sb_2O)M_6O_{18}$) (M = Mo, V, Nb) (○).

noticeable that MoO_2 is observed neither in Sb-containing catalysts nor in Te-containing materials probably because during the hydrothermal synthesis this oxide reacts with Te and Sb oxides leading to the formation of the multi-metal containing phases.

DR-UV–vis spectra of samples heat-treated at 450 °C or 600 °C are shown in Fig. 2. In the case of the MoVNbO catalysts, the DR spectra present two different regions at 200–450 nm and 500–700 nm (Fig. 2a). The assignation of oxidation states in the 200–450 nm range is a very difficult task because in this region the signals of many species converge, mainly V^{5+} (250–450 nm) [30,31], Mo^{6+} (250–400 nm) [32,33], and Nb^{5+} (235–310 nm) [34]. However, the bands observed in the 500–750 nm range are related to Mo and V in oxidation states lower than 6+ and 5+, respectively. Therefore, a maximum about 550–600 nm corresponds to the presence of Mo^{5+} [32,33], although its position can vary as this band overlaps with other multiple band in the range of 620–750 nm due to the presence of V^{4+} [30,31] or at ca. 510 nm due to V^{3+} [35]. In any case, the ratio between broad bands present in the 200–450 nm range and those present in the 500–800 nm range in sample A-450 is higher than in sample A-600. This suggests that the sample A-600 has Mo and/or V species with an average oxidation state lower than those in sample A-450.

DR-UV–vis spectra of Te- or Sb-containing catalysts are similar to those achieved in A-series, with the higher intensity of the broad bands in the 500–750 nm region in samples heat-treated at 600 °C. In this sense, previous ESR studies suggest the presence of Mo^{5+} and V^{4+} in these type of catalysts, i.e. MoVNbO [14], MoVSbO [36–38], MoVTeO and MoVTeNbO [39,40]. Thus, the differences between samples heat-treated at 450 °C and 600 °C are related not only to the development of crystalline phases (as determined by XRD) but also by the differences in the oxidation state of V and Mo, being apparently the average oxidation state lower in samples heat-treated at 600 °C.

On the other hand, no definitive assignment of the oxidation state of Te or Sb from the DR-UV–vis could be done, particularly, if we consider that Te and Sb possess very weak UV–vis absorption bands. Thus, bands at 195–230 nm (Sb^{3+}), 230–280 nm and 480 nm (Sb^{4+} and $Sb^{4.33+}$) and 300–340 nm (Sb^{5+}) could be observed for antimony species [41], while Te^{4+} and Te^{6+} present absorption maxima in the 250–300 nm range [42]. Nevertheless, previous XANES studies in the Sb L_I level shown that antimony remains mainly as Sb^{3+} when Mo–V–Sb mixed oxides are heat-treated in N_2 atmosphere [38], while XPS results indicate the presence of Sb^{3+} in MoVSbO [38] or Te^{4+} in MoVTeNbO [26,40,43] on the surface of catalysts.

As a brief summary, Mo–V–X (X = Nb, Sb, Te) mixed oxides heat-treated in N_2 at 450 °C or 600 °C present as main oxidation states Mo^{6+}/Mo^{5+}, V^{5+}/V^{4+}, Nb^{5+}, as well as Sb^{3+} or Te^{4+}, although the average oxidation state of Mo and V for samples heat-treated at 600 °C seems to be lower than those heat-treated at 450 °C.

Fig. 3 shows the results of the TPR experiments carried out with materials heat-treated at 450 °C and 600 °C. The H_2-consumption in TPR experiments of samples heat-treated at 450 °C is always higher than those obtained with samples calcined at 600 °C (Table 1), indicating that average oxidation state of samples heat-treated at 600 °C must be lower than those heat-treated at 450 °C. In addition, the H_2-uptake decreases according to the following trend: C- > B- > D- > A-series. However, an opposite trend is achieved when

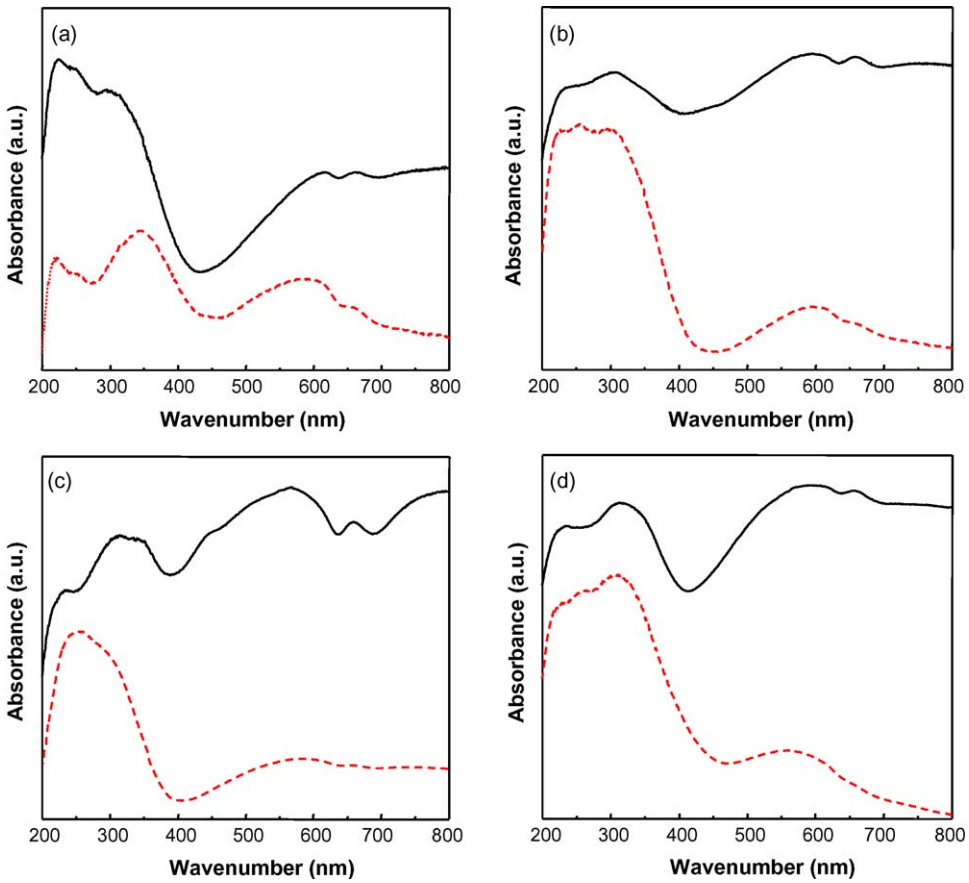

Fig. 2. Diffuse reflectance UV–vis spectra of catalysts: (a) A-series; (b) B-series; (c) C-series; (d) D-series, heat-treated at 450 °C (dashed line) or 600 °C (solid line).

considering the H_2-consumption at temperatures lower than 650 °C (i.e. excluding the decomposition of crystalline phases). Accordingly, the H_2-consumption was higher for Nb-containing samples than for Nb-free samples, suggesting that the average oxidation state and/or the reactivity of solid framework oxygen atoms in Nb-containing samples should be higher than Nb-free samples. This conclusion is in agreement to the DRS results, in which the appearance of bands in the 500–750 nm region, related to the presence of V (with oxidation state lower than 5+) or Mo (with oxidation state lower than 6+) was higher on samples heat-treated at 600 °C.

On the other hand, the TPR patterns indicate that the stability of the solid during TPR experiments also depends on both the catalyst composition and the final activation temperature. Thus, TPR patterns of MoVSbO catalysts, i.e. B-450 and B-600 samples (Fig. 3b), show a very sharp peak at 650–670 °C. This peak could be related to the decomposition of Mo–V–Sb phases which are metastable above 600 °C [22]. A similar peak is also observed in the TPR pattern of A-450 sample (although with lower intensity) but it is not observed in A-600 (Fig. 3a). Moreover, such peak is not observed in the TPR patterns of Te-containing materials, i.e., C- and D-series (respectively, Fig. 3c and d), although they present equivalent crystalline phases than those observed in the Sb-sample (M1 and M2). Accordingly, Te-containing materials show a thermal stability during the reduction step superior to the Sb-containing samples.

3.2. Catalytic results in ethane ODH

Fig. 4 shows the conversion of ethane and the selectivity to ethylene obtained during the oxidative dehydrogenation of ethane at 380 °C. In all cases, the only reaction products detected were ethylene, CO and CO_2. Results indicate that catalytic activity for catalysts heat-treated at 450 °C is always higher that for samples treated at 600 °C, the conversion decreasing as follows: C- ∼ B- >A- ∼ D-series, in an opposite trend to those observed for H_2-consumption in the TPR experiments or the catalyst surface areas, in which Nb-containing samples (A- and D-series) presented the higher H_2-uptake and the higher surface areas. According to these results it seems that catalysts with a lower average oxidation state as in Nb-free catalysts are more active in ethane activation than those Nb-containing catalysts.

On the other hand, the selectivity to ethylene is always higher for catalysts heat-treated at 600 °C (Fig. 4). Moreover, it is known that the selectivity to ethylene is seriously affected by ethane conversion. For this reason, it should be more appropriate to compare selectivity to ethylene at the same ethane conversion. According to the results in Fig. 5, the selectivity to ethylene decreases as follows: D- > C- ∼ B- ≫ A-series, being the selectivity to ethylene higher on the Nb-containing catalyst heat-treated at 600 °C and presenting M1 phase. So, the variation of the selectivity to ethylene with the ethane conversion depends not only on the presence/absence of M1 phase but also on the catalyst composition.

Scheme 1 shows the tentative reaction network for these catalysts. This is in agreement to previous results obtained in the ODH of ethane on Mo- and/or V-containing catalysts [9–23]. It has been reported that the selectivity to ethylene at low ethane conversions is related to the k_1/k_2 ratio while the selectivity to ethylene at high ethane conversions should be related to the $k_1/(k_2 + k_3)$ ratio. Results in Fig. 5 clearly suggest that steps 2 and 3 in Scheme 1 are favored on catalysts heat-treated at 450 °C but are less favored for samples Sb- or Te-containing samples calcined at

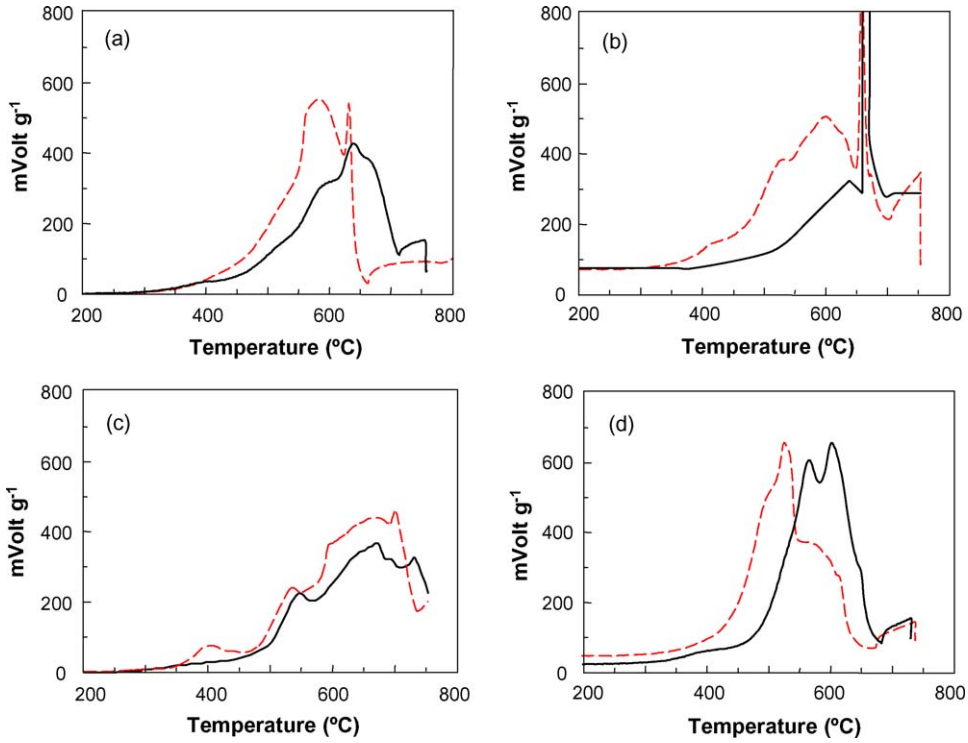

Fig. 3. TPR-H_2 patterns of catalysts: (a) A-series, (b) B-series, (c) C-series and (d) D-series. Samples heat-treated at 450 °C (dashed line) or 600 °C (solid line).

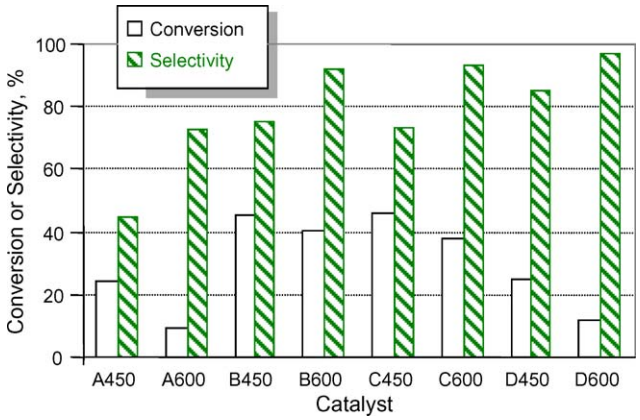

Fig. 4. Ethane conversion and selectivity to ethylene at 380 °C on mixed metal oxide catalysts. Contact time, W/F, of 40 g_{cat} h^{-1} $mol^{-1}_{C_2H_6}$.

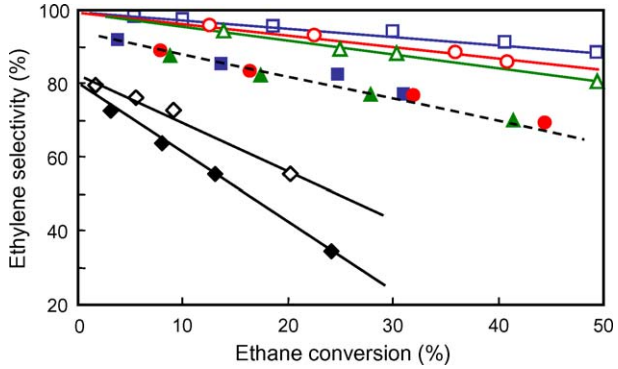

Fig. 5. Variation of the selectivity to ethylene with the ethane conversion obtained during the oxidation of ethane at 380 °C on mixed metal oxide catalysts: A-450 (◆); A-600 (◇); B-450 (▲); B-600 (△); C-450 (●); C-600 (○); D-450 (■); D-600 (□).

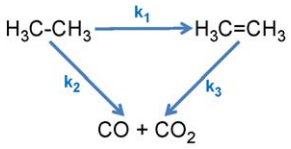

Scheme 1. Reaction network in ODH of ethane.

600 °C, especially for D-600 sample. Thus, we can conclude that the selective oxidative activation of ethane occurs in any case but ethylene combustion is partially favored at high ethane conversions over catalysts with amorphous or low crystalline phases (samples heat-treated at 450 °C). Moreover, a higher selectivity to ethylene is obtained on catalysts calcined at 600 °C (in which $(SbO)_2M_{20}O_{56}$ or $Te_2M_{20}O_{57}$ are mainly present), especially in the case of MoVTeNbO catalyst.

The presence of Te or Sb during the calcination step favors clearly the formation and stability of selective crystalline phases (M1-type) and the elimination of non-crystalline phases. This is of special importance in the case of Nb-containing catalyst. While MoO_2 and other non-stoichiometric oxides are observed in Mo–V–Nb–O, only M1 and M2 phases are observed in the Nb-containing MoVTeO catalyst. An excess of tellurium could facilitate the transformation of MoO_2 forming $TeMo_5O_{16}$ or other Te-containing bronzes, which are inactive in alkane oxidation [21,23,29,39].

4. Conclusions

Non-stoichiometric mixed oxides are observed in Mo–V–Nb–O based catalysts. However, the incorporation of Sb or Te in Mo–V(Nb)-based catalysts facilitates the development of the orthorhombic M1 phase in the range of 450–600 °C. The presence of these elements probably favors also the removing of non-selective crystalline phases, as MoO_2 (which is very active but not selective in the ethane oxidation). In this sense, the higher selectivity of Sb or

Te-containing catalysts in ethane ODH is due to: (i) a development of the orthorhombic phase M1; (ii) a removal of non-selective crystalline phases as MoO_2. However, since MoVTeNbO catalysts are more selective that MoVTeO or MoVSbO catalysts suggest that an additional factor should also be considered.

On the other hand, the catalytic activity seems to be related to the behavior of catalysts in the TPR experiments. Thus, this was higher on Nb-free samples which presented a low H_2-consumption in the TPR experiments. Accordingly, lower oxidation state of Mo and V species are required in order to achieve a higher catalytic activity for ethane oxidation.

Acknowledgements

Financial support from DGICYT in Spain through Project CTQ2006-09358/BQU is gratefully acknowledged. P. B. also thanks the program Ramón y Cajal from Spain.

References

[1] S. Alboneti, F. Cavani, F. Trifiró, Catal. Rev. -Sci. Eng. 38 (1996) 413.
[2] M.M. Bettahar, G. Costentin, L. Savary, J.C. Lavalley, Appl. Catal. A: Gen. 145 (1996) 1.
[3] T. Blasco, J.M. López Nieto, Appl. Catal. A 157 (1997) 117.
[4] M.M. Lin, Appl. Catal. A 207 (2001) 1.
[5] R.K. Grasselli, J.D. Burrington, D.J. Buttrey, P. DeSanto Jr., Cl.G. Lugmair, A.F. Volpe Jr., T. Weingand, Top. Catal. 23 (2003) 5.
[6] T. Ushikubo, Catal. Today 78 (2003) 43.
[7] D. Vitry, J.-L. Dubois, W. Ueda, J. Mol. Catal. A 220 (2004) 67.
[8] J.M. López Nieto, Top. Catal. 41 (2006) 3.
[9] E.M. Thorsteinson, T.P. Wilson, F.G. Young, P.H. Kasai, J. Catal. 52 (1978) 116.
[10] F.G. Young, E.M. Thorsteinson, U.S. Patent 4,250,346 (1983).
[11] J.H. McCain, U.S. Patent 4,524,236 (1985).
[12] M. Merzouki, B. Taouk, L. Monceaux, E. Bordes, P. Courtine, Stud. Surf. Sci. Catal. 72 (1992) 165.
[13] K. Ruth, R. Kieffer, R. Burch, J. Catal. 175 (1998) 16.
[14] D. Linke, D. Wolf, M. Baerns, O. Timpe, R. Schoegl, S. Zeyβ, U. Dingerdisen, J. Catal. 205 (2002) 16.
[15] W. Ueda, K. Oshihara, Appl. Catal. A 200 (2000) 135.
[16] P. Botella, J.M. López Nieto, A. Dejoz, M.I. Vázquez, A. Martínez-Arias, Catal. Today 78 (2003) 507.
[17] Y. Liu, P. Cong, R.D. Doolen, S. Guan, V. Markov, L. Woo, S. Zeyss, U. Dingerdissen, Appl. Catal. A 254 (2003) 59.
[18] T. Johann, A. Brenner, M. Schwickardi, O. Busch, F. Marlow, S. Schunk, F. Schuth, Catal. Today 81 (2003) 449.
[19] G. Grubert, E. Kondratenko, S. Kolf, M. Baerns, P. van Geem, R. Parton, Catal. Today 81 (2003) 337.
[20] J.M. López Nieto, P. Botella, M.I. Vázquez, A. Dejoz, Chem. Commun. (2002) 1906.
[21] P. Botella, E. García-González, A. Dejoz, J.M. López Nieto, M.I. Vázquez, J. González-Calbet, J. Catal. 225 (2004) 428.
[22] P. Botella, A. Dejoz, J.M. López Nieto, P. Concepción, M.I. Vázquez, Appl. Catal. A 298 (2006) 16.
[23] P. Botella, J.M. López Nieto, A. Dejoz, M.I. Vázquez, A. Martínez-Arias, Catal. Today 91–92 (2004) 241.
[24] E. García-González, J.M. López Nieto, P. Botella, J.M. González-Calbet, Chem. Mater. 14 (2002) 4416.
[25] J.M.M. Millet, M. Baca, A. Pigamo, D. Vitry, W. Ueda, J.L. Dubois, Appl. Catal. A 244 (2003) 359.
[26] J.M.M. Millet, H. Roussel, A. Pigamo, J.L. Dubois, J.C. Dumas, Appl. Catal. A: Gen. 232 (2002) 77.
[27] (a) P. De Santo, D.J. Buttrey, R.K. Grasselli, C.G. Lugmair, A.F. Volpe, B.H. Toby, T. Vogt, Top. Catal. 23 (2003) 23;
(b) P. De Santo, D.J. Buttrey, R.K. Grasselli, C.G. Lugmair, A.F. Volpe, B.H. Toby, T. Vogt, Z. Krystallogr. 219 (2004) 152.
[28] H. Tsuji, K. Oshima, Y. Koyasu, Chem. Mater. 15 (2003) 2112.
[29] P. Botella, E. García-González, J.M. López Nieto, J.M. González-Calbet, Solid State Sci. 7 (2005) 507.
[30] H. Aritani, T. Tanaka, T. Funabiki, S. Yoshida, K. Eda, N. Sotani, M. Kudo, S. Hasegawa, J. Phys. Chem. 100 (1996) 19495.
[31] T. Blasco, P. Concepción, J.M. López Nieto, J. Pérez-Pariente, J. Catal. 152 (1995) 1.
[32] V.R. Porter, W.B. White, R. Roy, J. Solid State Chem. 4 (1972) 250.
[33] (a) J.C.J. Bart, F. Cariati, A. Sgamelloti, Inorg. Chim. Acta 36 (1979) 105;
(b) J.C.J. Bart, G. Petrini, N. Giordano, Z. Anorg, Allg. Chem. 413 (1975) 180.
[34] J.M.R. Gallo, I.S. Paulino, U. Schuchardt, Appl. Catal. A 266 (2004) 223.
[35] F. Cavani, G. Centi, F. Trifiró, A. Vaccari, in: M. Che, G.C. Bond (Eds.), Adsoprtion and Catalysis on Oxide Surfaces, Elsevier, Amsterdam, 1985, p. 287.
[36] E.M. Novakova, J.C. Vedrine, E.G. Derouane, J. Catal. 211 (2002) 235.
[37] M. Baca, J.M.M. Millet, Appl. Catal. A: Gen. 279 (2005) 67.
[38] T. Blasco, P. Botella, P. Concepción, J.M. López Nieto, A. Martínez-Arias, C. Prieto, J. Catal. 228 (2004) 362.
[39] P. Botella, B. Solsona, A. Martinez-Arias, J.M. López Nieto, Catal. Lett. 74 (2001) 149.
[40] P. Botella, J.M. López Nieto, B. Solsona, A. Mifsud, F. Márquez, J. Catal. 209 (2002) 445.
[41] H. Matsumura, K. Okumura, T. Shimamura, N. Ikenaga, T. Miyake, T. Suzuki, J. Mol. Catal. A 250 (2006) 122.
[42] J.M. López Nieto, P. Botella, B. Solsona, J.M. Oliver, Catal. Today 81 (2003) 87.
[43] K. Asakura, K. Nakatani, T. Kubota, Y. Iwasawa, J. Catal. 194 (2000) 309.